

Exploring Performance Limits on Proactive Fair Scheduling for mmWave WLANs

Ang Deng, Yuchen Liu, and Douglas M. Blough
School of Electrical and Computer Engineering
Georgia Institute of Technology
Atlanta, GA 30332-0765

Abstract—Although the millimeter wave (mmWave) band has great potential to address ever-increasing demands for wireless bandwidth, its intrinsically unique propagation characteristics call for different scheduling strategies in order to minimize performance drops caused by blockages. A promising approach to mitigate the blockage problem is proactive scheduling, which uses blockage predictions to schedule users when they are experiencing good channel conditions. In this paper, we formulate an optimal scheduling problem with fairness constraints that allows us to find a schedule with maximum aggregate rate that achieves approximately the same fairness as the classic proportional fair scheduler. The results show that, for the problem settings studied, up to around 30% increase in aggregate rate compared to classic proportional fair scheduling (PFS) is possible with no decrease in fairness when blockages can be accurately predicted 0.5 seconds in advance. Furthermore, aggregate rate could be doubled compared to PFS if blockages can be accurately predicted 5 seconds in advance. While these results demonstrate the very promising potential of proactive scheduling, we also discuss several future research directions that must be pursued to effectively realize the approach.

Index Terms—mmWave, proactive scheduling, blockage

I. INTRODUCTION

The rapid increase in internet bandwidth demand has led to standards such as 5G and IEEE 802.11ad/ay, where utilization of the millimeter-wave (mmWave) spectrum is expected to deliver multi-Gbps performance. However, bandwidth alone does not guarantee performance for applications like Ultra High Definition (UHD) video, virtual/augmented reality, and cloud gaming. In fact, users' experiences for these applications can be severely impacted by any substantial drop in data rate, which can cause noticeable delay for live UHD video streaming or service failure for cloud gaming.

The distinct propagation characteristics of mmWave signals bring new challenges to all layers of the network stack. One of the most significant issues is that signal strength can be severely attenuated when blockage occurs along the line-of-sight path between access point (AP) and user equipment (UE) [1]–[3], which can cause sudden and large decreases in link data rates. This makes the timing of transmissions much more critical than in sub 6 GHz networks that have more stable link data rates, and therefore intelligent scheduling to avoid transmissions during poor channel condition times is crucially important for mmWave networks. A potentially promising approach is to combine blockage prediction with proactive

scheduling techniques in order to activate links when they are experiencing the best channel conditions, thereby maintaining the continuously high data rates necessary for applications like UHD video and virtual/augmented reality.

In this work, we study the potential benefits that can be provided by proactive scheduling that makes use of blockage prediction. We first formulate an optimal proactive scheduling problem with fairness constraints and show that it has the form of a binary integer linear programming (BILP) problem. This problem formulation allows us to use existing optimization software to explore the maximum aggregate rates achievable with proactive scheduling while maintaining proportional fairness. The results show that, for the problem settings studied, up to around 30% increase in aggregate rate compared to classic proportional fair scheduling (PFS) is possible with no decrease in fairness when blockages can be accurately predicted 0.5 seconds in advance. Furthermore, aggregate rate could be doubled compared to PFS if blockages can be accurately predicted 5 seconds in advance. These findings motivate future research on both efficient proactive scheduling techniques and improved blockage prediction, for example by integrating blockage prediction and mobility prediction.

The paper is organized as follows. Section II discusses related work. The system model we employ for this study is described in Section III. Section IV describes the methodology we used to formulate the optimal scheduling problem as a BILP problem. Section V presents numerical results along with their analysis. Lastly, Section VI concludes the work with key findings and a discussion of future work.

II. RELATED WORK

Proactive scheduling has been explored in non-mmWave wireless communications by many prior works, e.g. [4]–[6]. This prior work mainly considers proactive schedulers that are modifications of the popular proportional fair scheduler and their results consistently show that future channel knowledge has significant potential to improve throughput while maintaining or improving fairness. These non-mmWave proactive schedulers mainly focus on using channel state information (CSI) prediction. However, in mmWave bands, CSI prediction alone is not enough to maintain high performance due to the susceptibility of mmWave signals to blockage.

Some prior work has explored the use of blockage prediction for proactive resource allocation in mmWave net-

works [7]–[9]. These works make use of different approaches to the blockage prediction problem and have different network goals. For example, [7] focuses on optimizing the handover process through prediction of blockages and their duration using peripherals and geometry. This allows elimination of unnecessary handovers for short-term blockages and proactive early handovers to avoid outages from longer-term blockages. In [8], the use of camera images to predict blockages from pedestrian mobility is proposed, while [9] employs a deep neural network (DNN) approach to predict mmWave beams and blockages.

Two prior works focus specifically on blockage-aware scheduling for mmWave networks [10], [11]. The work in [10] tries to alleviate the severe service degradation experienced by UEs during a blockage by allocating time-slots to them early in the scheduling period before the blockage occurs. As with the earlier proactive schedulers, [10] is a modified version of the proportional fair scheduler. There is also work that combines blockage awareness with proactive scheduling in a more integrated fashion. For example, [11] proposes a DNN scheduler that combines blockage prediction with scheduling and beamforming. The goal of that work is maximizing UE achievable rate but fairness is not considered.

III. SYSTEM MODEL

As noted above, [10] is a closely related work in that it considers the same problem domain, namely blockage-aware proactive scheduling for mmWave networks. Thus, we adopt a system model that is based on the one from that prior work. In this model, there are n_U UEs located in a room where one mmWave access point (AP) is mounted on the ceiling. The AP employs the orthogonal frequency-division multiple access (OFDMA) scheme to transmit downlink data from an infinitely backlogged queue for a total duration of T ms and in time slots of length Δt . We divide the total duration into a number of scheduling sessions, each containing n_{ts} time slots. We refer to n_{ts} as the scheduling session length. We assume that the scheduler assigns all sub-carriers of a time-slot to the same UE, with an aggregate bandwidth b .

We also adopt the blockage model used in [10], [12]. In this model, UEs move between four states: LOS, DECAY, NLOS, and RISE. The NLOS and LOS states, respectively, indicate when the link between the AP and a UE is or is not obstructed by a blockage. The received power in the NLOS state is assumed to be a small fraction of the received power in the LOS state. The DECAY and RISE states describe the transitioning phases between the LOS and NLOS states. During the transition, the received power is assumed to vary linearly (on a dB scale) in between the LOS and NLOS received powers. We denote the decay factor (transition rate) from the LOS state to the NLOS state by ρ_D and the rise factor (transition rate) from the NLOS state to the LOS state by ρ_R . The possible state transitions are shown in Figure 1.

For each UE, we assume that blockage events occur following a Poisson distribution and the NLOS state duration is exponentially distributed. The blocker arrival rate is denoted

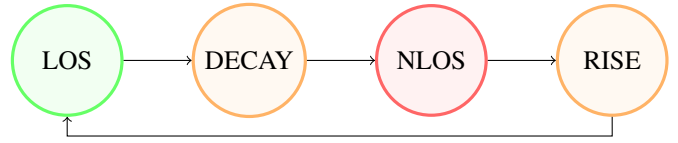


Fig. 1. Blockage model state transition diagram

by λ_B , and the mean blockage duration is denoted by τ_B . The distance between AP and UE is denoted by d_u . For our simulation results presented in Section V, the model above is used to determine the rates of each user in each slot as shown in the following equations. The UE received power p_{rx} is given by the following formula:

$$p_{rx} = \frac{p_{tx} \cdot g_{tx} \cdot g_{rx} \cdot l_0 \cdot d_u^{-\nu}}{A}, \quad (1)$$

where A is an attenuation factor that is equal to 1 in the LOS state, reaches a maximum value A_{max} in the NLOS state, and varies as noted above during the transition states. We then use Shannon's capacity to estimate the user data rate:

$$r = b \cdot \log_2 \left(1 + \frac{p_{rx}}{p_n} \right). \quad (2)$$

This rate is then used by the scheduling algorithms.

IV. METHODOLOGY

In order to explore the upper performance limits of what can be achieved with proactive fair scheduling, we define an optimal scheduling problem over a single scheduling session. We assume that the blockage condition of each node is accurately predicted within the scheduling session and the goal is to maximize aggregate data rate subject to fairness constraints. As we will show in the remainder of this section, this problem can be formulated as a Binary Integer Linear Programming (BILP) problem. The BILP problem can be solved with state-of-the-art optimization software to determine the maximum possible aggregate data rate under the given fairness constraints. In Section IV-A, we describe the optimization problem using a simple example for illustration purposes and in Section IV-B, we give the full problem formulation.

A. Basic Scheduling Problem Example

We first depict the scheduling problem in an assignment table to lay the foundation for understanding our formulation of the BILP problem. In Table I, we show a sample assignment schedule for a system with 2 users and 4 time-slots. Each value of 1 in the table indicates that the corresponding time-slot has been assigned to a particular user. In this example, time-slots 1, 3, and 4 are assigned to user 1 and time-slot 2 is assigned to user 2. A value of zero means that the user is not active in the corresponding time-slot.

TABLE I
EXAMPLE ASSIGNMENT TABLE FOR A 2 USER 4 TIME-SLOT SYSTEM

	TS 1	TS 2	TS 3	TS 4
User 1	1	0	1	1
User 2	0	1	0	0

In parallel, we have Table II with the same structure but showing the achievable rate for each user in each time-slot based on the predicted channel conditions. Multiplying these two tables element-wise and taking the average over all time-slots yields the predicted average data rate during this period, which for the example shown is 1.5 Gbps.

TABLE II
EXAMPLE PREDICTED RATES FOR A 2 USER 4 TIME-SLOT SYSTEM
(GBPS)

	TS 1	TS 2	TS 3	TS 4
User 1	1.2	0.8	1.2	2.1
User 2	0.4	1.5	1.2	0.8

It can be seen from Table I that in order for the schedule to be valid, there are two conditions that need to be met. First, the sum of each row indicates how many time-slots are assigned to this particular user, and these row sums need to add up to the number of total time-slots, which is 4 in this case. In our implementation, in order to guarantee comparable fairness with other scheduling algorithms as well as to prevent the algorithm from overly prioritizing UEs with favorable channel conditions, we take this requirement a step further and constrain each user to have a particular number of slots. As will be shown later, this approach allows our algorithm to achieve a certain fairness condition. Second, for each time-slot (column) there must be exactly one user to whom the time-slot is assigned. In other words, each column must sum to 1. It is also true that, if a table meets these two conditions, then it is a valid schedule, i.e. these conditions are necessary and sufficient for a schedule to be valid.

B. BILP Problem Formulation

In this part, we present how this scheduling problem is formulated into a BILP problem, with the goal being to maximize the sum rate over a single scheduling session with a given fairness constraint. The main constraints in our scheduling problem are:

- 1) there is exactly one user assigned in each time slot, and
- 2) a user u_i is assigned to exactly b_i time slots in the scheduling session under consideration.

The second constraint is what allows us to meet certain fairness criteria. To be specific, since we will compare the optimal scheduler to variations of the proportional fair scheduler, we will allocate to each user the same number of time slots it is allocated in the corresponding proportional fair scheduler. Thus, each user will get the same amount of time in the wireless channel as it gets in the corresponding proportional fair scheduler, which we consider to be achieving the same approximate fairness.¹

We begin the problem formulation by defining a column vector \mathbf{X} of size $n_U * n_{ts}$ which contains binary numbers

¹Note that the relative rates of different users will not be *exactly* the same for the optimal and proportional fair schedulers since the rates each user gets in its different time slots might differ across the two schedules. However, we will show in Section V that the fairness values of the optimal scheduler and a corresponding proportional fair scheduler are in fact very close in practice.

denoting whether a particular time-slot is assigned to a specific user (0 for not assigned and 1 for assigned). This assignment vector can be considered as an unwinding of Table I going in ascending time order and row by row. For example, the sample schedule in Table I would be represented by the vector [1 0 1 1 0 1 0 0]. Each of the values in the vector represents if the time-slot is assigned to the corresponding user, and it is interpreted that the first n_{ts} elements represents the assignment for user 1, and the second n_{ts} elements for user 2, etc. An assignment vector of this type is the output of our optimized scheduler.

Next, we construct a matrix \mathbf{A} of size $n_U + n_{ts}$ by $n_U * n_{ts}$. The first n_U rows denote the constraint that each user is only allowed a fixed number of time-slots. The last n_{ts} rows denote the constraint that only one user can be assigned in each time-slot. The exact construction of \mathbf{A} is as follows: let k be the row number, then for the first n_U rows, for each value of k , $a_{kq} = 1$ for $(k-1)*n_U < q \leq k*n_U$, and $a_{kq} = 0$ otherwise. For the last n_{ts} rows, for each value of k , $a_{kq} = 1$ for every n_{ts} th element starting from the $(k - n_U)$ th element in row, and $a_{kq} = 0$ otherwise. Matrix \mathbf{A} is only dependent on n_U and n_{ts} .

Finally, we define a column vector \mathbf{B} of length $n_U + n_{ts}$ that includes the b_i constraints. The first n_U rows equal the number of total time-slots to be allocated to each user and the last n_{ts} rows are all equal to 1.

To illustrate the matrix setup, if we have 2 users, 4 time-slots, and each user is allocated 2 time-slots, then the equation $\mathbf{AX} = \mathbf{B}$ is:

$$\begin{bmatrix} 1 & 1 & 1 & 1 & 0 & 0 & 0 & 0 \\ 0 & 0 & 0 & 0 & 1 & 1 & 1 & 1 \\ 1 & 0 & 0 & 0 & 1 & 0 & 0 & 0 \\ 0 & 1 & 0 & 0 & 0 & 1 & 0 & 0 \\ 0 & 0 & 1 & 0 & 0 & 0 & 1 & 0 \\ 0 & 0 & 0 & 1 & 0 & 0 & 0 & 1 \end{bmatrix} \begin{bmatrix} x_1 \\ x_2 \\ x_3 \\ x_4 \\ x_5 \\ x_6 \\ x_7 \\ x_8 \end{bmatrix} = \begin{bmatrix} 2 \\ 2 \\ 1 \\ 1 \\ 1 \\ 1 \end{bmatrix} \quad (3)$$

This equation ensures that any solution \mathbf{X} satisfies the aforementioned constraints and is therefore a valid schedule.

To implement the objective function, we construct a row vector \mathbf{R} whose elements have a 1-to-1 correspondence to vector \mathbf{X} , similar to how Table II is to Table I. The element values of \mathbf{R} are the achievable link rates as calculated in (2) for users in each time-slot. The product of \mathbf{RX} and Δt is the total amount of data that is transmitted in the total duration of $n_{ts} * \Delta t$ scheduled time (one scheduling session). Putting everything together, the optimization problem to maximize the aggregate rate across n_U UEs and n_{ts} time-slots with fairness constraints is given by the following BILP problem:

$$\begin{aligned} & \max \mathbf{RX} \\ & \text{s.t. } \mathbf{AX} = \mathbf{B} \end{aligned} \quad (4)$$

whereby the solution vector \mathbf{X} is an optimal schedule.

V. NUMERICAL RESULTS

In this section, a series of simulations are run in order to study the performance limits of proactive fair scheduling for mmWave networks with blockage prediction. We evaluate aggregate rates and fairness values of the classic proportional fair (PF) scheduler, the blockage-aware proportional fair (BA-PF) scheduler from [10], and the optimal scheduler produced by solving Problem (4). As mentioned earlier, in order to compare the aggregate rates while keeping approximately the same fairness values, we provide the time-slot allocations of the proportional fair schedulers as constraints to the optimal (denoted by BILP) scheduler. Note that, although PF and BA-PF are selected here for comparison, the time slot allocation can be any arbitrary division among users, e.g. another possibility would be to equally divide slots among users to achieve perfect time-based fairness. Our setup creates four scheduling results, denoted by: PF, BA-PF, BILP_{PF} , and $\text{BILP}_{\text{BA-PF}}$.

A. Simulation Setting

For experiments in Sections V-B through V-D, we simulate a total of 9 seconds of transmission time. In these results, this total time is divided into a number of scheduling sessions, where the scheduling session length, n_{ts} , is a parameter. Recall that we assume accurate prediction over one scheduling session so this allows us to evaluate how performance varies with prediction capability, i.e. how far ahead predictions can be made with good accuracy. In Sections V-B through V-D, we consider relatively short session lengths of 0.1 to 0.5 seconds, which is in the range of blockage prediction capability based solely on signal processing techniques. In Section V-E, we consider session lengths of 1 to 5 seconds. This can be considered as a “what if” experiment, where we investigate potential performance gains that could be achieved if accurate blockage predictions can be achieved farther ahead of time.

Lastly, in order to model possible prediction error, we insert a random variable $E \sim \mathcal{N}(0, \sigma^2)$ where $\sigma = 0.1$ into (2) to get the effective rate \hat{r} , and use \hat{r} in all algorithms being compared.

$$\hat{r} = b \cdot \log_2\left(1 + \frac{p_{rx} + E}{p_n}\right) \quad (5)$$

The fixed parameters used in this experiment are consistent with [10] and are listed in Table III. The AP is located at 2 meters height above all 8 UEs, and the UEs are uniformly distributed within a circular area of 15 meters radius horizontally from the AP. The optimizer applied to solve the BILP in this experimental study is the IBM ILOG CPLEX optimizer.

B. User Rate ECDF Comparison

In this set of experiments, mean blockage duration τ_B is set to be 1000 ms, the blocker arrival rate ranges from 0.25 to 1 blockers/sec. in step sizes of 0.25, and n_{ts} is set to be 8000, making each scheduling session 0.5 seconds long. The empirical cumulative distribution functions (ECDFs) of the four schedulers for different arrival rates are shown in Fig. 2.

For each of the subplots in Fig. 2, it can be observed that BILP_{PF} , and $\text{BILP}_{\text{BA-PF}}$ schedulers produce higher user

TABLE III
FIXED SIMULATION PARAMETERS

Bandwidth	b	2GHz
Noise power	p_n	-71.99dBm
Scheduling time slot length	Δt	62.5 μ s
Decay factor	ρ_D	0.2 dB/ms
Rise factor	ρ_R	6.7 dB/ms
Transmit power	p_{tx}	20dBm
Transmitter gain	g_{tx}	3.16dBi
Receiver gain	g_{rx}	0dBi
Path loss reference	l_0	63.4dB
Attenuation exponent	v	1.72
Maximum attenuation	A_{max}	40dB

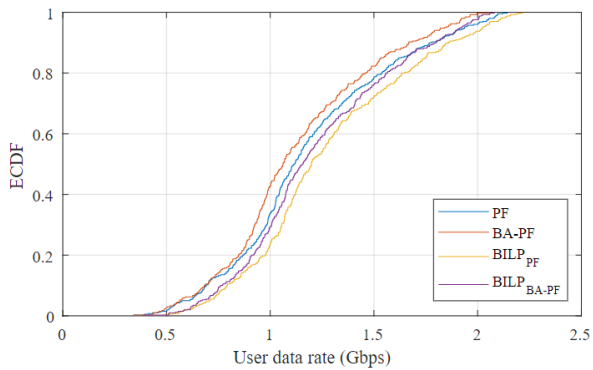
data rates as compared to the corresponding PF and BA-PF schedulers. In Fig. 2a, the BILP performance improvements are fairly uniform over different user data rates. As more blockages occur, which can be observed in Fig. 2b to Fig. 2d, the horizontal distance between non-BILP and BILP curves increases as the y-coordinate increases. This indicates that, even though the BILP scheduler improves UE data rate across all UEs, UEs in better channel conditions experience a larger absolute improvement than UEs in worse conditions. For example, in Fig. 2d, for the 10th percentile UE, the data rate difference between BILP_{PF} and PF is 0.1 Gbps and at the 90th percentile, the difference is 0.26 Gbps. The BILP and non-BILP curves are roughly parallel between the 20th and 80th percentile, indicating the improvement is fairly uniform for UEs with more typical channel conditions.

C. Average User Rate and Fairness Comparison

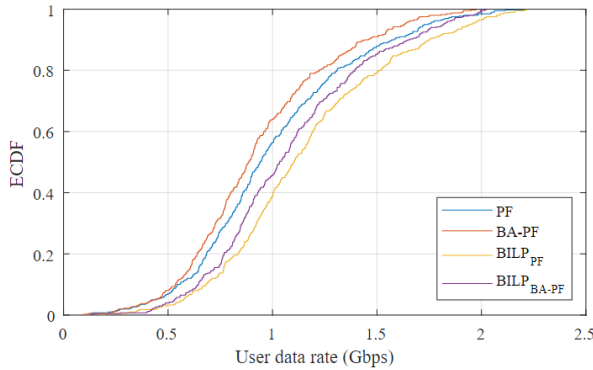
For the same setting as in Section V-B, Figure 3 shows the average data rate for the four schedulers. The figure shows that, as the blocker arrival rate increases, the difference between BILP and non-BILP schedulers increases. For example, as the blocker arrival rate increases from 0.25 blockers/sec. to 1 blocker/sec., the average user data rate percentage gain of BILP_{PF} over PF increases from 7.98% to 31.84%.² This shows that proactive scheduling based on blockage prediction has strong potential to improve overall performance, particularly in high blockage scenarios.

To verify that the performance improvement of BILP does not come at the expense of fairness, we also evaluated the sum of log rates of the different schedulers. It has been shown that achieving proportional fairness is equivalent to maximizing this metric [13]. This metric is plotted in Figure 4 for the four schedulers. Note the scale on the y-axis, which indicates that all four schedulers are actually very close to each other in terms of sum of log rates and, therefore, they all achieve approximately the same proportional fairness. Somewhat counterintuitively, however, the BILP schedulers actually do slightly better on this metric than the PF scheduler. This is explained by the fact that, in our model, the channel state distribution is non-stationary and it is well known that the PF algorithm does not perfectly maximize the sum of log rates in that scenario [5].

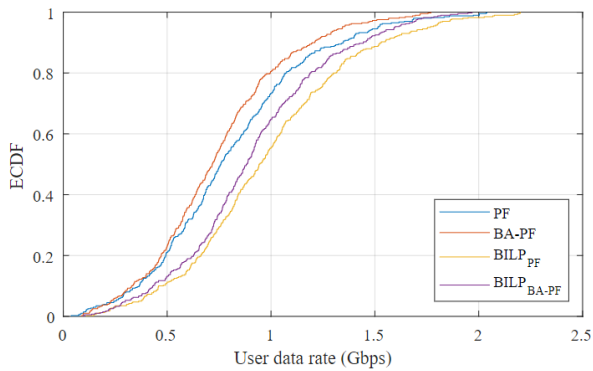
²There is an even larger difference between $\text{BILP}_{\text{BA-PF}}$ and BA-PF, because BA-PF's main goal is improving the performance of UEs at the lowest data rates, rather than overall performance.



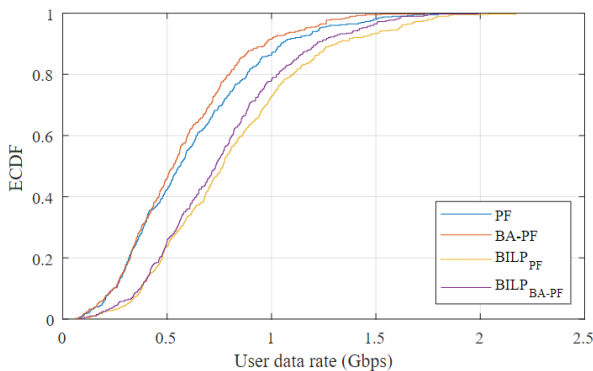
(a) $\lambda_B = 0.25$ blockers/s



(b) $\lambda_B = 0.5$ blockers/s



(c) $\lambda_B = 0.75$ blockers/s



(d) $\lambda_B = 1$ blockers/s

Fig. 2. ECDF Comparison

D. Impact of Scheduling Session Length

In this section, we evaluate the average user data rate as scheduling session length is varied. The parameter values are

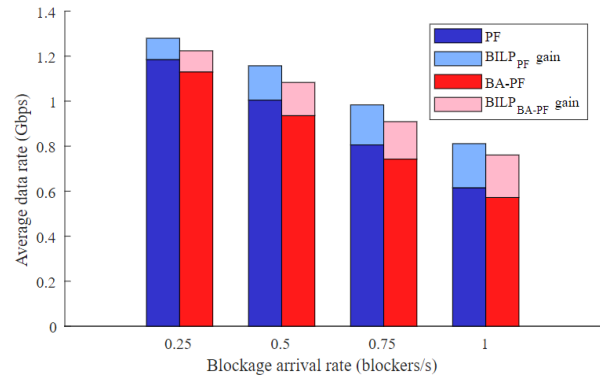


Fig. 3. Average user data rate vs. blocker arrival rate.

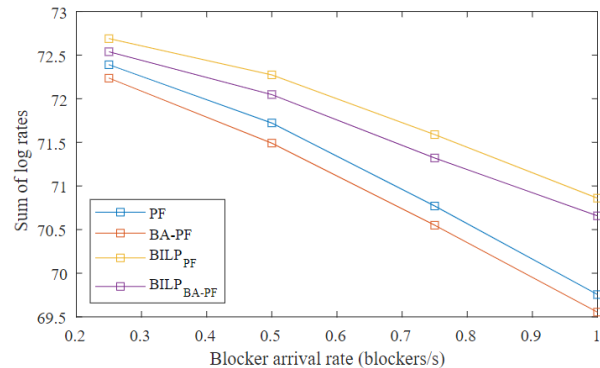


Fig. 4. Average sum of logarithmic user rates vs. blocker arrival rate.

the same as in Sections V-B and V-C, except that session length is a variable and blocker arrival rate is fixed at 0.75/sec. Figure 5 shows the average user data rate for the four schedulers as the scheduling session length is varied from 0.1 to 0.5 seconds. It is clear that the longer the scheduling session is, the more improvement there is for the optimal scheme. This is, as expected, due to having a larger pool of time-slots over which the schedule is optimized.

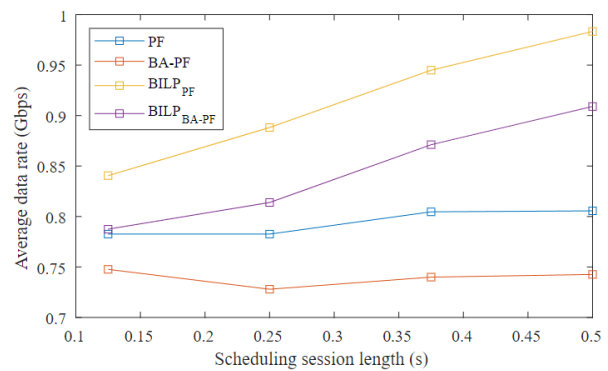


Fig. 5. Arrival rate 0.75 blockers/s,

E. Estimated Impact of Longer Scheduling Sessions

In this section, we extend the experiment of Section V-D to even longer scheduling sessions. Due to the limits of optimization software, however, we were not able to solve the BILP exactly for these session lengths. Instead, we used an approximate approach where we solved a modified BILP

with time slot aggregation. To be specific, each group of 10 time slots was considered as one virtual time slot in the BILP specification. Thus, the resulting "optimal" schedule has the same user scheduled for 10 consecutive real time slots.

In this experiment, we simulate a total of 90 seconds of transmission time and consider scheduling session lengths of 1 to 5 seconds. All other parameters are the same as in Section V-D. The results are shown in Figure 6. It is clear that even larger potential performance gains can be achieved with longer scheduling sessions (compare to Figure 5). For example, with a 5 second scheduling session, the modified BILP_{PF} achieves almost double the average data rate of the PF scheduler. Thus, if accurate blockage predictions can be done further in advance, there is enormous potential for performance improvement with blockage-aware scheduling.

As a side note, as the session length increases, BA-PF has better performance than PF, which differs from the results with shorter session lengths. This is likely due to BA-PF having greater temporal freedom to schedule users ahead of blockage occurrence, which is one of its main goals. Thus, increasing the time frame of blockage prediction also significantly benefits the BA-PF algorithm.

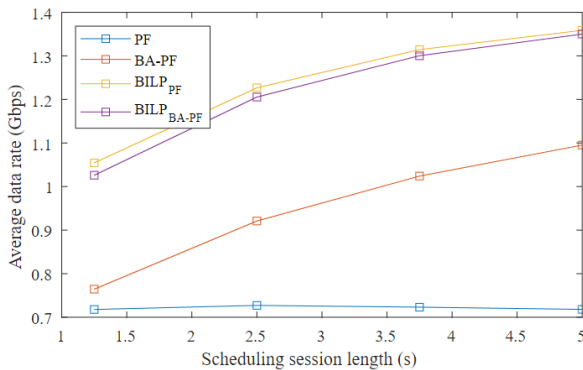


Fig. 6. Arrival rate 0.75 blockers/s, aggregated

VI. CONCLUSIONS

In this work, we formulated and solved an optimal scheduling problem in order to investigate the potential performance improvements of proactive schedulers that make use of blockage prediction. Results showed that, for the evaluated scenarios, up to about 30% higher aggregate rate over classic proportional fair scheduling can potentially be achieved with no degradation in fairness if blockage predictions are accurate 0.5 seconds in advance. Furthermore, extending blockage prediction lead times to 5 seconds can potentially double aggregate rate with no fairness loss.

We believe that these results motivate several interesting research directions. First, while the ILP solver approach yields upper limits on performance, it is clearly not practical. Thus, **it is important to develop fast schedulers that approximate the ILP solution if the potential of proactive scheduling is to be realized.** The BA-PF scheduler of [10] can be considered as a first attempt at this. However, results show that its benefits are somewhat limited with blockage prediction lead times of

0.5 seconds or less while it shows moderate performance gains with longer prediction lead times. Thus, more research is still needed on this topic. Second, if blockages can be predicted further in advance, the potential performance improvements of proactive scheduling increase dramatically. Thus, **developing longer-time-scale blockage prediction techniques is critically important.** With maps of static obstacles combined with mobility prediction of moving obstacles (primarily humans), we believe that this is a solvable problem, particularly in WLAN settings where the number of users in the same area is often not very large.

ACKNOWLEDGMENT

This research was supported in part by the National Science Foundation under Grant CNS-1813242.

REFERENCES

- [1] H. Zhao, R. Mayzus, S. Sun, M. Samimi, J. K. Schulz, Y. Azar, K. Wang, G. N. Wong, F. Gutierrez, and T. S. Rappaport, "28 GHz millimeter wave cellular communication measurements for reflection and penetration loss in and around buildings in New York City," in *2013 IEEE International Conference on Communications (ICC)*, 2013, pp. 5163–5167.
- [2] G. R. MacCartney, S. Deng, S. Sun, and T. S. Rappaport, "Millimeter-wave human blockage at 73 GHz with a simple double knife-edge diffraction model and extension for directional antennas," in *2016 IEEE 84th Vehicular Technology Conference (VTC-Fall)*, 2016, pp. 1–6.
- [3] Y. Liu and D. M. Blough, "Analysis of blockage effects on roadside relay-assisted mmwave backhaul networks," in *ICC 2019-2019 IEEE International Conference on Communications (ICC)*. IEEE, 2019, pp. 1–7.
- [4] H. J. Bang, T. Ekman, and D. Gesbert, "Channel predictive proportional fair scheduling," *IEEE Transactions on Wireless Communications*, vol. 7, no. 2, pp. 482–487, 2008.
- [5] R. Margolies, A. Sridharan, V. Aggarwal, R. Jana, N. K. Shankaranarayanan, V. A. Vaishampayan, and G. Zussman, "Exploiting mobility in proportional fair cellular scheduling: Measurements and algorithms," *IEEE/ACM Transactions on Networking*, vol. 24, no. 1, pp. 355–367, 2016.
- [6] L. Shen, T. Wang, and S. Wang, "Proactive proportional fair: A novel scheduling algorithm based on future channel information in OFDMA systems," in *2019 IEEE/CIC International Conference on Communications in China (ICCC)*, 2019, pp. 925–930.
- [7] J. Bao, T. Shu, and H. Li, "Handover prediction based on geometry method in mmWave communications: A sensing approach," in *2018 IEEE International Conference on Communications Workshops (ICC Workshops)*, 2018, pp. 1–6.
- [8] K. Y. Y. Oguma, T. Nishio and M. Morikura, "Proactive handover based on human blockage prediction using RGB-D cameras for mmWave communications," *IEEE Transactions on Mobile Computing*, vol. E99-B, no. 6, pp. 1734–1744, Oct. 2016.
- [9] M. Alrabeiah and A. Alkhateeb, "Deep learning for mmWave beam and blockage prediction using sub-6 GHz channels," *IEEE Transactions on Communications*, vol. 68, no. 9, pp. 5504–5518, 2020.
- [10] F. Firyaguna, A. Bonfante, J. Kibilda, and N. Marchetti, "Performance evaluation of scheduling in 5G-mmWave networks under human blockage," *CoRR*, vol. abs/2007.13112, 2020. [Online]. Available: <https://arxiv.org/abs/2007.13112>
- [11] F. Götsch and M. Kaneko, "Deep learning-based beamforming and blockage prediction for sub-6-GHz/mmWave mobile networks," in *GLOBECOM 2020 - 2020 IEEE Global Communications Conference*, 2020, pp. 1–6.
- [12] G. R. MacCartney, T. S. Rappaport, and S. Rangan, "Rapid fading due to human blockage in pedestrian crowds at 5G millimeter-wave frequencies," in *GLOBECOM 2017 - 2017 IEEE Global Communications Conference*, 2017, pp. 1–7.
- [13] H. Kim and Y. Han, "A proportional fair scheduling for multicarrier transmission systems," *IEEE Communications Letters*, vol. 9, no. 3, pp. 210–212, 2005.